Available online at www.sciencedirect.com
SCIENCE DIRECT®
Biochimica et Biophysica Acta 1655 (2004) 93–101
BIOCHIMICA ET BIOPHYSICA ACTA
BBA
www.bba-direct.com

Review

Modulation of the free energy of the primary quinone acceptor (Q_A) in reaction centers from *Rhodobacter sphaeroides*: contributions from the protein and protein–lipid(cardiolipin) interactions

Laszlo Rinyu[a], Erik W. Martin[b], Eiji Takahashi[b], Péter Maróti[a], Colin A. Wraight[b,*]

[a] *Department of Biophysics, University of Szeged, Hungary*
[b] *Department of Biochemistry, and Center for Biophysics and Computational Biology, University of Illinois, USA*

Received 24 April 2003; received in revised form 23 July 2003; accepted 23 July 2003

Abstract

The redox midpoint potential (E_m) of Q_A, the primary quinone of bacterial reaction centers, is substantially modulated by the protein environment. Quite subtle mutations in the Q_A binding site, e.g., at residues M218, M252 and M265, cause significant increases in the equilibrium constant for electron transfer to Q_B, which indicate relative lowering of the E_m of Q_A. However, reports of functional linkage between the Q_A and Q_B sites make it difficult to partition such effects between Q_A and Q_B from purely relative changes. We report here measurements on the yield of delayed fluorescence emission from the primary donor (P) accompanying the thermally activated charge recombination of $P^+Q_A^-$ to form the excited singlet state of the primary donor, P*. The results show that for mutations of the Q_A site residues, Met^{M218} and Ile^{M265}, essentially all the substantial thermodynamic effect is localized at Q_A, with no evidence for a significant effect of these residues on the properties of Q_B or the mutual influence (linkage) of Q_A and Q_B. We also report a significant lowering of the E_m of Q_A by the native lipid, cardiolipin, which brings the E_m in isolated reaction centers more in line with that seen in native membrane vesicles (chromatophores). Possible origins of this effect are discussed in the context of the Q_A binding site structure.

Keywords: Photosynthetic reaction center; Electron transfer; Quinone; Cardiolipin; Midpoint redox potential; Delayed fluorescence

1. Introduction

The acceptor quinones of bacterial reaction centers, Q_A and Q_B, perform the function of accumulating two reducing equivalents from one-electron turnovers of the primary photoevents. After two turnovers, Q_B is doubly reduced and the quinol is released from the Q_B site, which is refilled by an oxidized quinone from the membrane pool [1–3]. Q_A^- is the reductant of both Q_B and Q_B^-, and the electrochemical properties of Q_A and Q_B must be suitably matched to allow this. In many cases, Q_A and Q_B are chemically identical, e.g., both are ubiquinone-10 in *Rhodobacter* (*Rba.*) *sphaeroides*, and the distinct physical properties of Q_A and Q_B, including redox potential, are controlled by interactions with the binding site environment.

The kinetics and energetics of electron transfer between the two quinones also exhibit distinct differences when measured in vivo versus in vitro (see, e.g., Refs. [4–7]), suggesting influences of the native membrane environment on the thermodynamic and kinetic properties of the primary and secondary acceptor quinones, Q_A and Q_B. The removal of cofactors during purification of the reaction center (RC) could potentially shoulder the blame for some of the differences that are manifest in kinetic measurements. Recent crystal structures of RCs from *Rba. sphaeroides* have shown that electron density previously modelled as detergent actually represents a well-defined cardiolipin bound on the surface of the reaction center, suggesting specific protein–lipid interactions [8,9]. The cardiolipin headgroup is situated such that it has contact with all three subunits, and is approximately 18 Å from both Q_A and Q_B. We report here that addition of cardiolipin to isolated reaction centers does indeed affect the properties and reactions of the quinones.

In investigating the origins of the redox properties of the bound quinones, we have found that seemingly subtle

* Corresponding author. Center for Biophysics and Computational Biology/MC147, University of Illinois, 607 South Mathews Avenue, Urbana, IL 61801, USA. Tel.: +1-217-333-3245; fax: +1-217-244-6615.
E-mail address: cwraight@uiuc.edu (C.A. Wraight).

0005-2728/$ - see front matter © 2004 Elsevier B.V. All rights reserved.
doi:10.1016/j.bbabio.2003.07.012

alterations in the Q_A binding site of *Rba. sphaeroides* can induce substantial changes in the redox midpoint potential (E_m) of the quinone. For example, mutation of residue M265 from isoleucine to the smaller, polar residues of serine and threonine caused a large decrease (80–110 mV) in the E_m of Q_A [10]. No effect was seen when Ile^{M265} was replaced by valine. Similar effects on the E_m were observed with either native Q-10 or 9,10-anthraquinone acting as Q_A, so the mechanism does not involve the conformation of the methoxy substituents of ubiquinone. However, the changes in redox potential of the native ubiquinone as Q_A were determined indirectly from the equilibrium constant for electron transfer from Q_A^- to Q_B, and, since the Q_A and Q_B sites are known to be functionally linked [11], this measurement is not without ambiguity. To establish the large magnitude of the effect of polar substitutions of Ile^{M265}, we have now carried out delayed fluorescence measurements on these, and other RCs with different mutations in the Q_A site, to determine the free energy of the Q_A/Q_A^- couple relative to the excited state of the primary electron donor.

2. Methods and Materials

The mutagenesis procedures, growth conditions for mutant cells, as well as the RC preparation procedure, have been described previously [10,12,13]. All expression strains used are derived from the green, carotenoid-containing strain Ga of *Rba. sphaeroides*, which is of wild-type constitution apart from terminal steps of the carotenoid synthesis pathway. The M265 mutations were obtained following the procedure of Kunkel [12,14]. Replacement of Ile^{M265} by serine, threonine and valine, respectively, yielded mutants M265IS, M265IT and M265IV. Mutations at M218 were obtained by the QuickChange site-directed mutagenesis system (Stratagene), and expressed in a light harvesting deletion background derived from the Ga strain, lacking both the *puc* and *puf* operons. In the expression vector, which was based on pRK415, the *puf* operon was inserted but with the coding regions of *puf* A and B deleted (E. Takahashi, unpublished). Replacement of Met^{M218} by alanine and glycine yielded mutants M218MA and M218MG.

Acceptor quinone functions were assayed by the kinetics of charge recombination (back reaction) and electron transfer, performed on a spectrophotometer of local design. Back reaction of the charge-separated states, $P^+Q_A^-$ and $P^+Q_AQ_B^-$, was determined from the P^+ decay kinetics monitored at 430 nm. The kinetics of the first electron transfer were measured at 397 nm, a wavelength that discriminates between the electrochromic responses to Q_A^- and Q_B^- [15,16].

The kinetics of the second electron transfer were measured as the disappearance of the semiquinone signal at 450 nm after the second flash, in the presence of ferrocene to rereduce P^+ after the first flash [17]. Ferrocene was added at concentrations from 4 to 200 μM, such that the rate of donation to P^+ was either much slower than the second electron transfer (at low pH) or much faster (at high pH).

Sample conditions for all measurements were 1–2 μM RCs, 0.02% Triton X-100, 0.5 mM each of Mes, Mops, Tricine, Ches, and Caps, 100 mM NaCl. 100 μM terbutryn was added for assays of Q_A activity, and 20 μM ubiquinone (Q-10) was added when required for Q_B activity. When present, cardiolipin (Sigma Corp., St. Louis) was added from a stock solution (5 mg/ml) in ethanol. Molar concentrations of cardiolipin were calculated on the basis of a molecular weight of 1480, appropriate for a fatty acid composition dominated by 18:1 chains.

Delayed fluorescence measurements were performed as described by Turzó et al. [18]. Reaction center function of each sample was characterized by the near-infrared absorbance spectrum and by measurement of the flash-induced P^+ signal amplitude and $P^+Q_A^-$ recombination kinetics before and after the lengthy delayed fluorescence measurement. Absorbance spectroscopy was performed on a kinetic spectrophotometer of local design. The free energy drop from P* to $P^+Q_A^-$, ΔG_{P^*A}, was calculated by comparison of the delayed and prompt fluorescence yields, according to Arata and Parson [19]:

$$\frac{\int F_d(t)\mathrm{d}t}{\int F_p(t)\mathrm{d}t} = \frac{k_f \phi_p}{k_d \phi_f} \exp(\Delta G_{P^*A}/k_B T)$$

$\int F_d(t)\mathrm{d}t$ and $\int F_p(t)\mathrm{d}t$ are the integrated intensities of delayed and prompt fluorescence, measured in the same sample but at very different excitation intensities (both in the linear region) to give similar emission intensities. $\int F_d(t)\mathrm{d}t$ is determined by a one-exponential fit to the decay of the delayed fluorescence signal; $\int F_p(t)\mathrm{d}t$ is determined by electronic integration of the prompt fluorescence, using a time constant (0.1 s) similar to that of the delayed fluorescence decay time. k_f is the radiative rate constant for reaction center bacteriochlorophyll (approx. 8×10^7 s^{-1}, from the Strickler–Berg relationship [19]), ϕ_p is the quantum yield of charge separation (effectively 1.0 [20]), k_d is the rate of decay of the delayed fluorescence signal (essentially the rate of decay of $P^+Q_A^-$, or k_P—see below), ϕ_f is the prompt fluorescence yield of P* in reaction centers ($4.0 \pm 1.5 \times 10^{-4}$ [21]).

It should be noted that there are systematic errors associated with the determination of ΔG_{P^*A} from delayed fluorescence. These arise from the use of an exponential fit to the decay of the emission. The $P^+Q_A^- \rightarrow PQ_A$ decay kinetics are not strictly exponential [22], although the deviation at room temperature is very small. Nevertheless, the choice of window over which the delayed fluorescence is fitted, as may be determined by the opening time of the photomultiplier shutter, does affect the numerical outcome. This probably accounts for the (small) discrepancies in ΔG_{P^*A} values reported in the literature, which range from 860 to 910 meV, at pH 8.0 [19,23]. However, providing a consistent protocol is employed, results are highly reproducible and allow good comparisons between different samples.

3. Results

3.1. Delayed fluorescence from $P^+Q_A^-$ in wild-type reaction centers

The parent (wild-type) strain for all the mutants studied, is the green, carotenoid-containing Ga strain, referred to here as GaWT, rather than the blue-green, carotenoidless R26 strain. These are identical with respect to reaction center proteins, but R26 reaction centers lack a bound carotenoid. Isolated RCs from these two ''wild-type'' strains appear to be functionally and thermodynamically almost identical. This is further indicated by the delayed fluorescence measurements shown here. Fig. 1 shows the free energy gap between P* and $P^+Q_A^-$ for GaWT to be indistinguishable from that of R26:

$$\Delta G_{P*A} = -890 \pm 5 \text{ meV (interpolated at pH 8.0)}$$

and with very similar pH dependence. The free energy gap in the true wild-type strain, 2.4.1, is also the same as that for R-26, at pH 8.0 (K. Turzó and P. Maróti, unpublished).

3.2. Delayed fluorescence from $P^+Q_A^-$ in mutant reaction centers

The ΔG_{P*A} values for all mutants are summarized in Table 1.

Table 1
ΔG_{P*A} for various Q_A-site mutant RCs (interpolated at pH 8.0)

GaWT	M265IV	M265IS	M265IT	M218MA	M218MG	M252WF
− 890	− 890	− 830	− 775	− 835	− 805	− 860 (meV)

3.2.1. M265 mutant reaction centers

M265IV mutant RCs exhibited almost unaltered delayed fluorescence, compared to GaWT, in the physiological pH range ($\Delta G_{P*A} = -890 \pm 10$ meV, interpolated at pH 8.0), but with a somewhat flatter pH dependence (Fig. 1). At pH 10.5 ΔG_{P*A} for M265IV RCs was 20 meV more negative than for GaWT RCs.

In contrast, the two polar M265 mutants gave substantially higher delayed fluorescence emission intensity, indicating a much smaller energy gap between P* and $P^+Q_A^-$, consistent with a significantly more negative redox potential for Q_A (Fig. 1). The calculated values, interpolated at pH 8.0, showed:

M265IS $\Delta G_{P*A} = -830 \pm 10$ meV

M265IT $\Delta G_{P*A} = -775 \pm 5$ meV

Compared to wild-type RCs, these values correspond to shifts in the E_m of Q_A of − 60 and − 115 mV, respectively.

For comparison with functional and FTIR studies performed in D_2O [24], we measured delayed fluorescence for wild-type and M265IS mutant RCs in D_2O. No significant

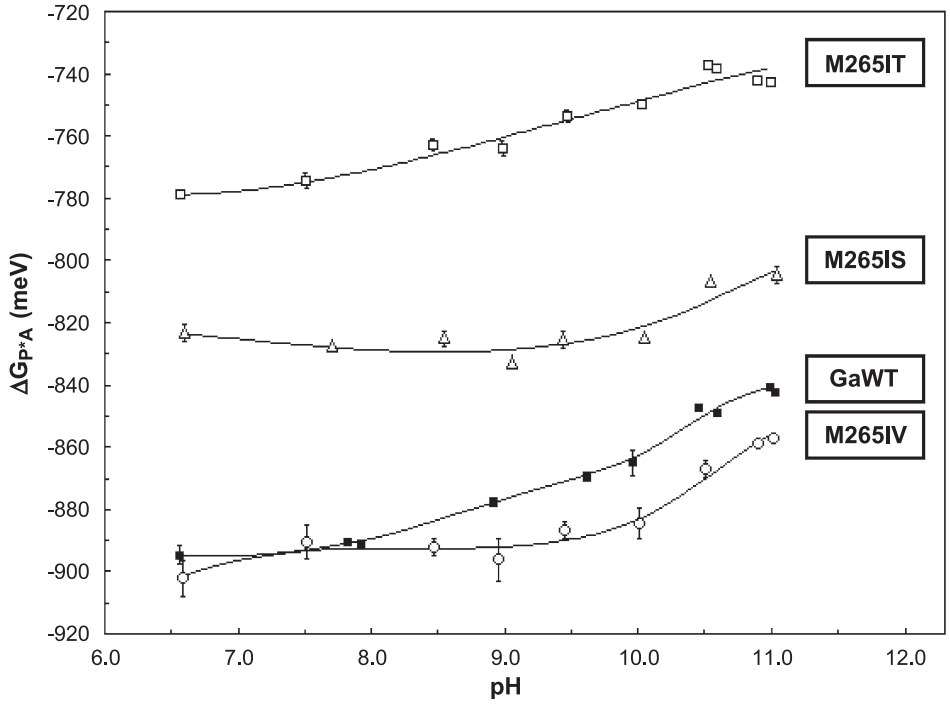

Fig. 1. The free energy drop from P* to $P^+Q_A^-$ in mutants at residue M265 of the Q_A binding site. ΔG_{P*A} was determined from the intensity of delayed fluorescence, as described in Methods and Materials. Conditions: 1–2 μM RCs, 0.02% Triton X-100, 2.5 mM buffer (0.5 mM of each of Mes, Mops, Tricine, Ches, and Caps), 100 mM NaCl, 100 μM terbutryn. From top to bottom: $Ile^{M265} \rightarrow$ Thr mutant RCs (M265IT), $Ile^{M265} \rightarrow$ Ser mutant RCs (M265IS), wild-type RCs (GaWT), $Ile^{M265} \rightarrow$ Val mutant RCs (M265IV).

effects of solvent isotope composition were observed between pH/pD 7 and 10.5. For M265IS, at pH/pD 9.8, paired measurements in H_2O and D_2O yielded $\Delta G_{P*A} = -830$ meV and $\Delta G_{P*A} = -829$ meV, respectively.

3.2.2. M218 mutant reaction centers

The two M218 mutant RCs gave substantially enhanced emission of delayed fluorescence. The calculated free energy gaps, interpolated at pH 8.0, were:

M218MA $\Delta G_{P*A} = -835 \pm 20$ meV

M218MG $\Delta G_{P*A} = -805 \pm 10$ meV

These values indicate E_m shifts for Q_A of -55 and -85 mV, respectively. Both M218 mutants showed qualitatively similar pH dependencies to those of GaWT and the M265 mutants (not shown).

3.2.3. M252 mutant reaction centers

Mutation of Trp^{M252} to phenylalanine also gave significantly enhanced emission of delayed fluorescence (Fig. 2). At pH 8.0, the free energy gap was determined to be:

M252WF $\Delta G_{P*A} = -860 \pm 10$ meV

3.3. Acceptor quinone function in M218 mutant reaction centers

The kinetic features of the M218 mutant RCs are summarized in Table 2.

3.3.1. The $P^+Q_A^- \rightarrow PQ_A$ back reaction

In the absence of a secondary donor to re-reduce P^+, back reaction of the charge-separated state, $P^+Q_A^-$, was monitored as P recovery at 430 nm. In wild-type RCs, the apparent rate constant, k_P^A, is about 9 s^{-1}, at room temperature. In both M218 mutants this rate was accelerated — $k_P^A = 27$ s^{-1} for M218MA, and $k_P^A = 38$ s^{-1} for M218MG (Table 2).

3.3.2. The $P^+Q_B^- \rightarrow PQ_B$ back reaction

With excess Q-10 present to reconstitute Q_B activity, the rate of P recovery from the $P^+Q_AQ_B^-$ state (apparent rate constant k_P^B) is significantly slower than from $P^+Q_A^-$, e.g., $k_P^B \approx 0.8$ s^{-1} in wild-type, at pH 8.0. The observed rate of decay was significantly slower in M218MA and M218MG mutant RCs: $k_P^B = 0.40$ s^{-1} and 0.22 s^{-1}, respectively, at pH 8.0 (Table 2). In comparison to the much faster decay from the $P^+Q_A^-$ state, this is indicative of a large equilibrium constant for electron transfer to Q_B (see below).

Table 2
Electron transfer characteristics of M218 mutant RCs (at pH 8.0)

	k_P^A (s^{-1})	k_P^B (s^{-1})	$L_{AB}^{(1)}$	$k_{AB}^{(1)}$ (s^{-1})	$k_{AB}^{(2)}$ (s^{-1})
GaWT	9.5	0.8	10	4×10^3	10^3
M218MA	27	0.4	65	4×10^3	2×10^3
M218MG	38	0.22	172	4×10^3	2×10^3

3.3.3. The first electron transfer: $Q_A^-Q_B \rightarrow Q_AQ_B^-$

The overall rate[1] of the first electron transfer was $k_{AB}^{(1)} = 4 \times 10^3$ s^{-1} in both M218 mutant RCs at pH 8.0 (Table 2). This is identical to the rate measured in wild-type RCs. However, the pH dependence of the rate was affected in the M218 mutant RCs, with onset of pH dependence at pH 8.5, 0.5–1 pH unit lower than in the wild-type (not shown).

3.3.4. The second electron transfer: $Q_A^-Q_B^- \rightarrow Q_AQ_BH_2$

The rate of the second electron transfer was 2-fold greater than in wild-type RCs, over the whole pH range examined (pH 5–11) (not shown).

3.4. Effects of lipids on acceptor quinone function in isolated reaction centers

3.4.1. The $P^+Q_B^- \rightarrow PQ_B$ back reaction

Addition of cardiolipin to isolated RCs in detergent suspension caused a significant slowing of the back reaction (charge recombination) of $P^+Q_B^-$. The effect showed half saturation at about 10–20 μM cardiolipin (not shown). Since the major route for recombination is via the $P^+Q_A^-$ state [16,25,26], this is indicative of a larger equilibrium constant for the one electron transfer, $Q_A^-Q_B \leftrightarrow Q_AQ_B^-$. With 100 μM cardiolipin, at pH 8.0, the slowing was approximately 3-fold, consistent with a 30 meV increase in the free energy drop from Q_A^- to Q_B. The effect was constant across the pH range, from pH 6 to 10.5 (not shown). The relative amplitude of the slow phase of the back reaction also increased from 70% to >90% in the presence of cardiolipin, indicating a substantial increase in the functional occupancy of the Q_B site.

The effect of cardiolipin titrates in with a half maximal effect at about 15 μM, indicating quite tight binding. However, a proper evaluation of the affinity cannot be made without a quantitative examination of the influence of the lipid/detergent ratio. Phosphatidylglycerol had a qualitatively similar effect of slowing the recombination rate, but the magnitude was smaller (<2-fold) even at the highest concentrations tested (200 μM). Phosphatidylcholine had no effect.

3.4.2. The second electron transfer, $Q_A^-Q_B^- \rightarrow Q_AQ_BH_2$

Cardiolipin caused a small, but consistent acceleration in the kinetics of the second electron transfer. The rate constant, $k_{AB}^{(2)}$, increased 1.5–2-fold over a wide pH range, from pH 6 to 10.5 (not shown). Although small, this change is consistent with expectations for this reaction, which is known to exhibit a Marcus-type free-energy dependence [27].

[1] The kinetics of the first electron transfer are not simple, and have at least two components, with characteristic times on the order of 30 and 300 μs. The relative amplitudes of the phases are variable and the origins of this multiphasicity are still controversial. The "overall" rate constant given here is derived from a single exponential fit to the kinetics, as generally reported in the past.

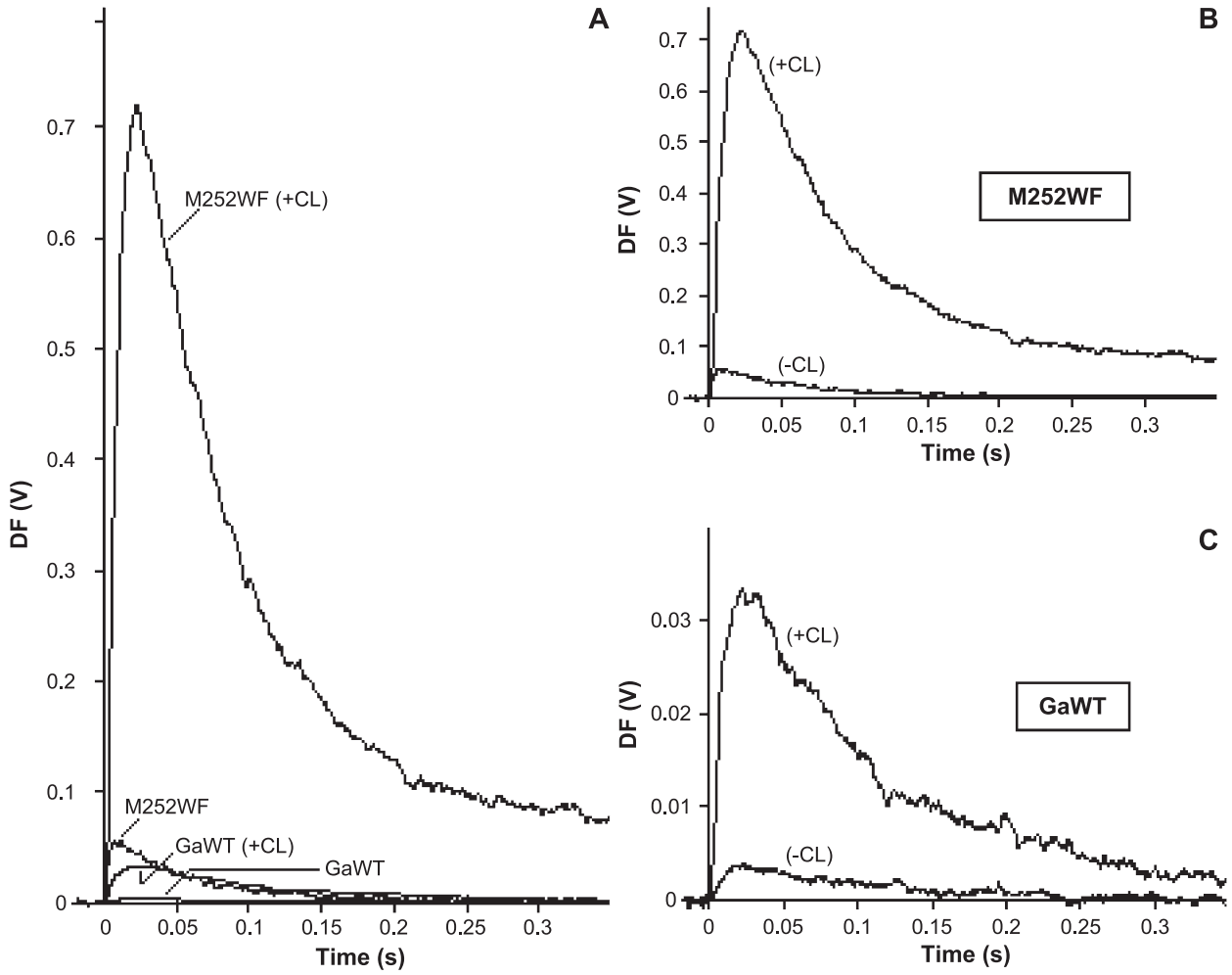

Fig. 2. The effect of cardiolipin on the delayed fluorescence emission (DF) from RCs. Wild-type RCs (GaWT) (A and C) and $Trp^{M252} \rightarrow Phe$ mutant RCs (M252WF) (A and B), with (+CL) and without (−CL) cardiolipin. Note the different vertical scales (volts) in all three panels. Conditions as for Fig. 1, with 100 μM cardiolipin (CL) where indicated.

3.4.3. Delayed fluorescence from $P^+Q_A^-$

The intensity of delayed fluorescence from wild-type RCs with terbutryn added, was increased 5–7-fold in the presence of cardiolipin (Fig. 2). Comparison of the integrated intensities showed the magnitude of ΔG_{P^*A} to decrease by 30 ± 10 meV. A similar emission enhancement by cardiolipin was seen in M252WF mutant RCs, equivalent to a decrease in the free energy change of 50 ± 10 meV. This estimate may be more reliable than that for wild-type RCs, due to the larger signal in this mutant.

4. Discussion

4.1. M265 mutant reaction centers

Substitution of the native isoleucine at position M265 with the small polar residues, serine and threonine, causes a substantial increase in the equilibrium constant, $L_{AB}^{(1)}$, for the one-electron transfer $Q_A^-Q_B \leftrightarrow Q_AQ_B^-$ [10]. This is consistent with a shift in the E_m of Q_A to lower potentials but, with native ubiquinone, the magnitude of the change could only be given lower limits of −50 and −80 mV for M265IS and M265IT mutant RCs, respectively. With anthraquinone as Q_A, the E_m of Q_A could be determined independently, and the polar mutants were found to have 80 and 105 mV lower potentials, respectively, for M265IS and M265IT, compared to GaWT RCs. The delayed fluorescence measurements reported here confirm that the effect on Q_A is quantitatively similar for both ubiquinone and anthraquinone. They also establish that essentially all the effect is on Q_A, with little or none on Q_B.

The delayed fluorescence intensity from the $P^+Q_A^-$ state in carotenoid-containing RCs of the GaWT strain revealed an essentially identical free energy gap, ΔG_{P^*A}, between P* and $P^+Q_A^-$ as for the carotenoidless strain, R26. Similarly, the M265IV mutant was indistinguishable from

the GaWT parent strain, at pH 8.0. However, for the polar mutants, ΔG_{P^*A} was 60 meV less negative for M265IS and 115 meV less negative for M265IT, at pH 8.0. These compare well with the estimated shifts in the E_m of Q_A of −80 mV for M265IS and −105 mV for M265IT, at pH 8.0, determined from the $P^+Q_A^-$ recombination kinetics with anthraquinone as Q_A [10].

We previously suggested that the substantial change in E_m of Q_A seen in the polar M265 mutants arises from subtle changes in the lengths of the hydrogen bonds to quinone carbonyls, especially C1=O [24]. It was proposed that the hydroxyl group of the serine and threonine side chains is hydrogen bonded to the peptide carbonyl of M261, pushing away the extended backbone region of M259–262. Energy minimization of the M265 mutant structures indicated a consequent lengthening of the hydrogen bond between C1=O of Q_A and the peptide nitrogen of M260, thereby destabilizing the semiquinone state.

The differences between the E_m shifts determined from delayed fluorescence with ubiquinone and the $P^+Q_A^-$ recombination kinetics with anthraquinone are certainly within the expected error margin. However, the discrepancies are in opposite directions for the two mutants, and may well reflect real distinctions based on the different side chain volumes or preferred rotamers of serine and threonine, as discussed previously [24]. This could allow subtle movements and consequent changes in the electronic coupling elements of the charge recombination reactions.

In a study of the infrared spectra associated with the Q_A and Q_A^- states of GaWT and the M265 mutant RCs, we observed that the semiquinone anion band was substantially affected in the mutant RCs. Furthermore, the spectrum of the polar mutants was unusually sensitive to D_2O, in contrast to GaWT and M265IV mutant RCs [24]. We considered it possible, but unlikely, that this could reflect a change in the hydrogen bond strength to one or both of the quinone oxygens. H/D exchange does not commonly affect hydrogen bond strength, but it is possible if the bonding potential is sufficiently anharmonic. Since hydrogen bonding to the quinone and semiquinone states is considered to contribute to establishing the functional redox potential of Q_A, a change in hydrogen (H/D) bond strength in D_2O should manifest itself in a change in ΔG_{P^*A}. We found here, however, that the free energy gap for M265IS mutant RCs was identical in H_2O and D_2O.

4.1.1. M218 mutant reaction centers

The $P^+Q_A^-$ back reaction kinetics are significantly faster for both M218 mutants than for wild-type RCs. In the wild-type, with ubiquinone as Q_A, the recombination process is by direct tunneling from Q_A^- to P^+ (k_{AP}) [28]. However, as the redox potential of Q_A is lowered, e.g., by mutation, a thermally activated route via P^+I^- becomes accessible (I is the bacteriopheophytin, $Bphe_A$, active in the primary charge separation pathway):

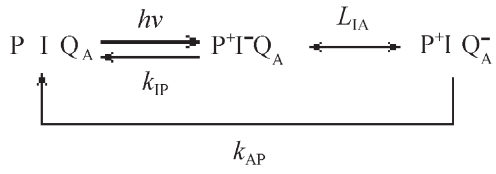

Significant contribution from this additional route results in acceleration of the overall rate of recombination, k_P^A. As previously discussed for the M265 polar mutants [10], it was likely that the faster rate of $P^+Q_A^-$ decay in the M218 mutants indicated a substantially lower E_m of Q_A, but the magnitude of the E_m shift could not be reliably determined from the native (ubiquinone) $P^+Q_A^-$ decay kinetics alone. However, the $P^+Q_B^-$ decay kinetics also reflect the Q_A midpoint potential, via the equilibrium constant, $L_{AB}^{(1)}$. According to the following scheme, $L_{AB}^{(1)}$ can be assayed from the charge recombination kinetics [1]:

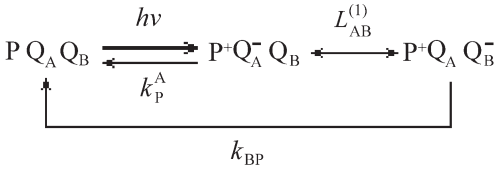

The rate constant for the direct route (k_{BP}) is small and has been estimated to be 0.1–0.12 s^{-1} in wild-type RCs [29], and 0.04–0.06 s^{-1} in L213DN mutant RCs where aspartic acid at position L213 is replaced by asparagine [13]. This is 100 times smaller than k_P^A and k_{BP} can sometimes be ignored—so long as $L_{AB}^{(1)}$ is not too large. Under such circumstances, comparison of the observed decays of $P^+Q_A^-$ and $P^+Q_B^-$, k_P^A and k_P^B, can be used as a simple and direct assay of $L_{AB}^{(1)}$ according to Ref. [1,26]:

$$L_{AB}^{(1)} \approx k_P^A / k_P^B - 1$$

This is adequate for wild-type RCs, where $L_{AB}^{(1)} \approx 10$ and k_P^B is about 10 times larger than k_{BP}. However, application of this approach to the M218 mutant RCs yields values of $L_{AB}^{(1)} = 65$ and 172, respectively, for M218MA and M218MG. As for the M265 polar mutants discussed above, these values are sufficiently large that they are likely to be underestimates, and they therefore correspond to minimum values for the change in the free energy gap from Q_A to Q_B of −35 and −70 meV.

The delayed fluorescence measurements confirm that significant shifts in the E_m of Q_A occur in the M218 mutant RCs (Table 1), and allow more definite values to be assigned. The magnitude of ΔG_{P^*A} decreased by 55 meV

for M218MA and 85 meV for M218MG, at pH 8.0. These values compare well with the lower limits determined from the increase in the $Q_A^- Q_B \leftrightarrow Q_A Q_B^-$ equilibrium constant (35 and 70 meV).

The structural basis for the substantial effect of the M218 mutations is not known at this time. The substituted residues, alanine and glycine, are very much smaller than the native methionine, which closes off one side of the Q_A pocket and contributes to the packing between Q_A and $Bphe_A$ (Fig. 3). It is possible that the small side chain volume of the mutant residues allows sequestration of one or more water molecules close to the quinone. The latter may be supported by preliminary data on anthraquinone-substituted RCs (E. Takahashi, unpublished), which suggest that the E_m shift in these mutants with anthraquinone as Q_A is significantly smaller than for the native ubiquinone. This might indicate that the larger anthraquinone moiety fills more of the available space than does ubiquinone.

4.1.2. Functional linkage between Q_A and Q_B

The fact that the effects of the Q_A site mutations at M218 and M265 are very largely localized to the thermodynamic properties of Q_A is not surprising. However, it is also not inevitable, as several observations indicate that the Q_A and Q_B sites interact in a manner that represents functional linkage [3,11]. Most notably, the chemical identity of the quinone in the Q_A site can affect the stoichiometry of proton uptake coupled to Q_A^- formation. Substitution of the native ubiquinone-10 with small naphthoquinones, e.g., 1,4-naphthoquinone or menadione (2-methyl naphthoquinone), eliminates proton uptake in the high pH region, pH>8.5 [30] (these analogues did not support detectable Q_B function). In this region, proton binding is considered to be primarily to residues that are located in or near the Q_B binding domain [31,32]. This is supported by site-directed mutation of the Q_B site residue, L212, from glutamic acid to glutamine, which also eliminates proton uptake in the high pH region [33,34].

We previously suggested that methionine M218 might have a role in this inter-site linkage, as it is in contact with the edge of the Q_A headgroup and could conceivably transmit steric interactions to the Q_B site via histidine M219 and the iron histidine complex that ligates both quinones [11]. However, the reasonable agreement between the change in the $Q_A^- Q_B \leftrightarrow Q_A Q_B^-$ electron transfer equilibrium and the decrease in ΔG_{P^*A} for the two M218 mutants suggests that the effects of these mutations are essentially localized to Q_A with little or no additional effect on Q_B.

4.1.3. M252 mutant reaction centers

The negative shift in the E_m of Q_A in response to mutating Trp^{M252} indicates that the interaction between the tryptophan and the quinone headgroup stabilizes the semiquinone state relative to the quinone. This is consistent with previous studies which have implicated Trp^{M252} in two important aspects of Q_A function. It appears to contribute to the electronic coupling between the bacteriopheophytin intermediate acceptor ($Bphe_A$ or I) and Q_A, necessary to achieve the normal, wild-type electron transfer rate of about $5 \times 10^{10}\ s^{-1}$ in *Rba. sphaeroides* [35] and *Rba. capsulatus* [36]. It is also involved in the binding of Q_A, as suggested by the close van der Waals contacts between the indole and the quinone rings. Mutation of tryptophan to tyrosine and phenylanine decreased the rate of electron transfer by factors of 3 and 5, respectively [35]. This change is sufficiently small that a subtle increase in distance could account for it, but the much greater (14-fold) slowing seen when leucine was substituted (in *Rba. capsulatus* [37]), supports the idea of an electronic effect. Mutation of Trp^{M252} also decreases the occupancy of the Q_A site after isolation of the RCs, but good occupancy can be recovered with excess ubiquinone in the tyrosine and phenylanine mutants. In contrast, we have been unable to restore workable levels of Q_A activity in isolated RCs of the Trp → Leu mutant, using ubiquinone (Q-10) (E. Takahashi, unpublished observations). The previous studies on similar

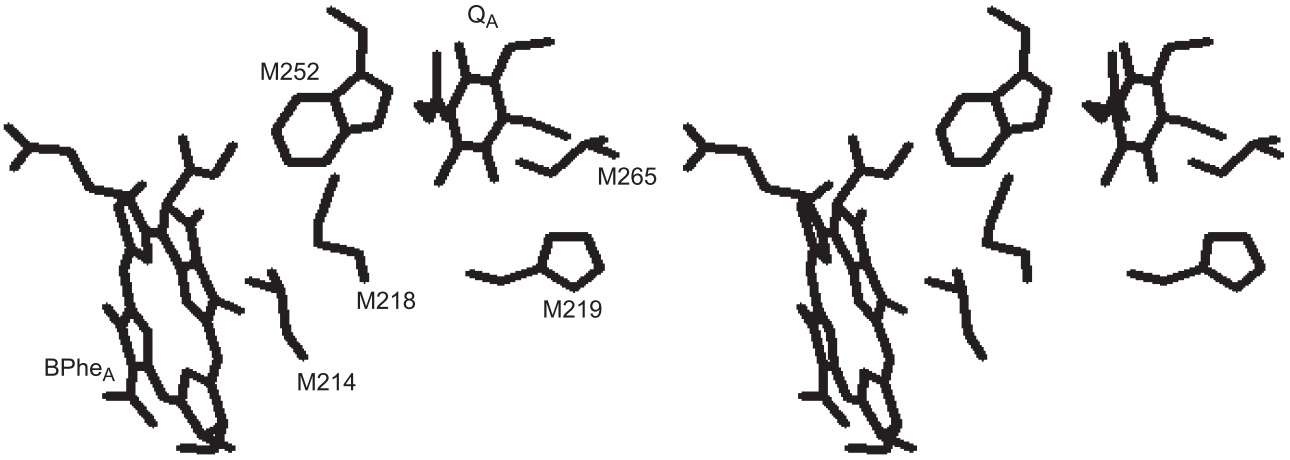

Fig. 3. Cross-eyed stereoview of the Q_A binding region showing the position of methionine M218 relative to Q_A and $Bphe_A$. Residues shown are: M214 (leucine), M218 (methionine), M219 (histidine), M252 (tryptophan), M265 (isoleucine).

mutants in *Rba. capsulatus* achieved reconstitution with menadione (2-methyl-1,4-naphthoquinone) [36,37].

4.2. The effect of cardiolipin on the redox potential of Q_A

Recent X-ray structures have shown one molecule of cardiolipin in a specific binding interaction with isolated RCs [8,9], and at least two other lipids are also seen to be associated with isolated RCs in a structurally defined manner [9]. Cardiolipin (diphosphatidylglycerol) is a negatively charged lipid with four acyl chains. The RC crystal structures locate the cardiolipin headgroup on the cytoplasmic side of the membrane, and in contact with all three subunits. The primary and secondary quinones are both approximately 1.8 nm from the cardiolipin headgroup.

The increased delayed fluorescence yield from $P^+Q_A^-$ and slowing of the $P^+Q_B^-$ back reaction by low levels of cardiolipin show that this lipid lowers the E_m of Q_A by 30–40 mV. Thus, although the cardiolipin observed in X-ray structures is positioned roughly equidistant from Q_A and Q_B, the effect of this lipid is exerted entirely through Q_A. The effect on Q_A is not large, but it is sufficient to account for a significant part of the larger Q_A/Q_B electron transfer equilibrium constant seen in native membranes compared to isolated RCs. Furthermore, quite small changes in the $Q_A^-Q_B \leftrightarrow Q_AQ_B^-$ free energy can have functionally significant effects via the quantum yield, since Q_A^- states are effectively blocked and the equilibrium constant is not large in this organism.

Since the cardiolipin observed in X-ray structures is evidently tightly bound, it would seem unlikely that the effect described here is related to this defined interaction site. However, the effect on the E_m of Q_A titrates in with significant affinity ($\approx$ 10 μM) and the cardiolipin content of RCs is apparently variable (L. Utschig, S. Schlesselman, D. Tiede, pers. comm.). Thus, the relatively small magnitude of the E_m shift could indicate only a partial effect due to partial occupancy of the site by endogenous lipid. If the X-ray-defined site is involved, it is noteworthy that although the cardiolipin observed in X-ray structures is positioned roughly equidistant from Q_A and Q_B, the effect of this lipid is exerted entirely through Q_A. Furthermore, the cardiolipin is bound to the protein surface at a location associated with the membrane/water interphase, where the dielectric constant is not expected to be small. Thus, the influence of the lipid on Q_A is unlikely to be electrostatic, and this is made clear by the lack of effect on Q_B over an essentially equal distance.

We therefore considered that the effect could be via the specific cardiolipin–protein interactions, revealed by the X-ray structures. These show cardiolipin to interact rather intimately with arginine-M267 in the interhelical loop that comprises the Q_A-binding site. Arg^{M267} also forms a salt bridge with Glu^{M263} that straddles M265, mutation of which has substantial effects on Q_A, as also reported here. The salt bridge may contribute to stabilizing the top of transmembrane helix E of the M subunit (helices D and E are the anchor points for the Q_A binding loop motif). However, preliminary data on a mutant, $Arg^{M267} \rightarrow$ Leu (kindly provided by M.R. Jones and P. Fyfe, Bristol, UK) indicate that the cardiolipin effect on Q_A/Q_B electron transfer equilibrium is very similar in the mutant RCs (E. Martin, unpublished data). This suggests that cardiolipin exerts its effect on Q_A through other means, such as interactions at other specific, but weaker, lipid binding sites.

Acknowledgements

This work was supported by a grant from the National Science Foundation (MCB99-05672) and a NSF-OTKA International Collaborative Grant (042) research supplement. P.M. thanks the Fulbright Association for a fellowship.

References

[1] V.P. Shinkarev, C.A. Wraight, Electron and proton transfer in the acceptor quinone complex of reaction centers of phototrophic bacteria, in: J. Deisenhofer, J.R. Norris (Eds.), The Photosynthetic Reaction Center, vol. 1, Academic Press, San Diego, 1993, pp. 193–255.

[2] M.Y. Okamura, G. Feher, Proton-coupled electron transfer reactions of Q_B in reaction centers from photosynthetic bacteria, in: R. Blankenship, M. Madigan, C. Bauer (Eds.), Advances in Photosynthesis, vol. 2, Kluwer Academic Publishing, Dordrecht, The Netherlands, 1995, pp. 577–593.

[3] C.A. Wraight, Proton and electron transfer in the acceptor quinone complex of bacterial photosynthetic reaction centers, Front. Biosci. 9 (2004) 309–337.

[4] P.L. Dutton, J.S. Leigh, C.A. Wraight, Direct measurement of the midpoint potential of the primary electron acceptor in *Rhodopseudomonas sphaeroides* in situ and in the isolated state: some relationships with pH and *o*-phenathroline, FEBS Lett. 36 (1973) 169–173.

[5] C.A. Wraight, Oxidation-reduction physical chemistry of the acceptor quinone complex in bacterial photosynthetic reaction centers: evidence for a new model of herbicide activity, Isr. J. Chem. 21 (1981) 348–354.

[6] A. Verméglio, Electron transfer between primary and secondary electron acceptors in chromatophores and reaction centers of photosynthetic bacteria, in: B.L. Trumpower (Ed.), Function of Quinones in Energy Conserving Systems, Academic Press, New York, 1982, pp. 169–180.

[7] J. Lavergne, C. Matthews, N. Ginet, Electron and proton transfer on the acceptor side of the reaction center in chromatophores of *Rhodobacter capsulatus*: evidence for direct protonation of the semiquinone state of Q_B, Biochemistry 38 (1999) 4542–4552.

[8] K.E. McAuley, P.K. Fyfe, J.P. Ridge, N.W. Isaacs, R.J. Cogdell, M.R. Jones, Structural details of an interaction between cardiolipin and integral membrane protein, Proc. Natl. Acad. Sci. U. S. A. 96 (1999) 14706–14711.

[9] A. Camara-Artigas, D. Brune, J.P. Allen, Interactions between lipids and bacterial reaction centers determined by protein crystallography, Proc. Natl. Acad. Sci. U. S. A. 99 (2002) 11055–11060.

[10] E. Takahashi, T.A. Wells, C.A. Wraight, Protein control of the redox potential of the primary acceptor quinone in reaction centers from *Rhodobacter sphaeroides*, Biochemistry 40 (2001) 1020–1028.

[11] C.A. Wraight, Functional linkage between the Q_A and Q_B sites of photosynthetic reaction centers, in: G. Garab (Ed.), Photosynthesis: Mechanisms and Effects, vol. II, Kluwer Academic Publishing, Dordrecht, 1998, pp. 693–698.
[12] E. Takahashi, P. Maróti, C.A. Wraight, Site-directed mutagenesis of *Rhodobacter sphaeroides* reaction center: the role of tyrosine L222, in: M. Baltscheffsky (Ed.), Current Research in Photosynthesis, vol. 1, Kluwer Academic Publishing, Dordrecht, 1990, pp. 169–172.
[13] E. Takahashi, C.A. Wraight, Proton and electron transfer in the acceptor quinone complex of *Rhodobacter sphaeroides* reaction centers: characterization of site-directed mutants of the two ionizable residues, Glu^{L212} and Asp^{L213}, in the Q_B^--binding site, Biochemistry 31 (1992) 855–866.
[14] T.A. Kunkel, Rapid and efficient site-specific mutagenesis without phenotypic selection, Proc. Natl. Acad. Sci. U. S. A. 82 (1985) 488–492.
[15] A. Verméglio, R.K. Clayton, Kinetics of electron transfer between the primary and secondary electron acceptor in reaction centers from *Rhodopseudomonas sphaeroides*, Biochim. Biophys. Acta 461 (1977) 159–165.
[16] C.A. Wraight, Electron acceptors of bacterial photosynthetic reaction centers: II. H^+ binding coupled to secondary electron transfer in the quinone acceptor complex, Biochim. Biophys. Acta 548 (1979) 309–327.
[17] P. Maróti, C.A. Wraight, Flash-induced H^+ binding by bacterial reaction centers: influences of the redox states of the acceptor quinones and primary donor, Biochim. Biophys. Acta 934 (1988) 329–347.
[18] K. Turzó, G. Laczkó, P. Maróti, Delayed fluorescence study on $P^*Q_A \rightarrow P^+Q_A^-$-charge separation energetics linked to protons and salt in reaction centers from *Rhodobacter sphaeroides*, Photosynth. Res. 55 (1998) 235–240.
[19] H. Arata, W.W. Parson, Delayed fluorescence from *Rhodopseudomonas sphaeroides* reaction centers: enthalpy and free energy changes accompanying electron transfer from P870 to quinones, Biochim. Biophys. Acta 638 (1981) 201–209.
[20] C.A. Wraight, R.K. Clayton, The absolute quantum efficiency of bacteriochlorophyll photooxidation in reaction centers, Biochim. Biophys. Acta 333 (1973) 246–260.
[21] K.L. Zankel, D.W. Reed, R.K. Clayton, Fluorescence and photochemical quenching in photosynthetic reaction centers, Proc. Natl. Acad. Sci. U. S. A. 61 (1968) 1243–1249.
[22] B.H. McMahon, J.D. Müller, C.A. Wraight, G.U. Nienhaus, Electron transfer and protein dynamics in the photosynthetic reaction center, Biophys. J. 74 (1998) 2567–2587.
[23] K. Turzó, G. Laczkó, Z. Filius, P. Maróti, Quinone-dependent delayed fluorescence from reaction centers of photosynthetic bacteria, Biophys. J. 79 (2000) 14–25.
[24] T.A. Wells, E. Takahashi, C.A. Wraight, Protein control of the redox potential of the primary quinone acceptor in reaction centers from *Rhodobacter sphaeroides*, Biochemistry 42 (2003) 4064–4074.
[25] D. Kleinfeld, M.Y. Okamura, G. Feher, Electron transfer in reaction centers of *Rhodopseudomonas sphaeroides*: I. Determination of the charge recombination pathway of $D^+Q_AQ_B^-$ and free energy and kinetic relations between $Q_A^-Q_B$ and $Q_AQ_B^-$, Biochim. Biophys. Acta 766 (1984) 126–140.
[26] C.A. Wraight, R.R. Stein, Bacterial reaction centers as a model for photosystem II: Turnover of the secondary acceptor quinone, in: Y. Inoue, A.R. Crofts, Govindjee, N. Murata, G. Renger, K. Satoh (Eds.), The Oxygen Evolving System of Photosynthesis, Academic Press, New York, 1983, pp. 383–393.
[27] M.S. Graige, M.L. Paddock, J.M. Bruce, G. Feher, M.Y. Okamura, Mechanism of proton-coupled electron transfer for quinone (Q_B) reduction in reaction centers of *Rb. sphaeroides*, J. Am. Chem. Soc. 118 (1996) 9005–9016.
[28] M.R. Gunner, D.E. Robertson, P.L. Dutton, Kinetic studies on the reaction center protein from *Rhodopseudomonas sphaeroides*: the temperature and free energy dependence of electron transfer between various quinones in the Q_A site and the oxidized bacteriochlorophyll dimer, J. Phys. Chem. 90 (1986) 3783–3795.
[29] A. Labahn, J.M. Bruce, M.Y. Okamura, G. Feher, Direct charge recombination from $D^+Q_AQ_B^-$ to DQ_AQ_B in bacterial reaction centers from *Rhodobacter sphaeroides* containing low potential quinone in the Q_A site, Chem. Phys. 97 (1995) 355–366.
[30] L. Kálman, P. Maróti, Stabilization of reduced primary quinone by proton uptake in reaction centers of *Rhodobacter sphaeroides*, Biochemistry 33 (1994) 9237–9244.
[31] E. Alexov, M.R. Gunner, Calculated protein and proton motions coupled to electron transfer: electron transfer from Q_A^- to Q_B in bacterial photosynthetic reaction centers, Biochemistry 38 (1999) 8254–8270.
[32] M.Y. Okamura, M.L. Paddock, M.S. Graige, G. Feher, Proton and electron transfer in bacterial reaction centers, Biochim. Biophys. Acta 1458 (2000) 148–163.
[33] P. Maróti, D.K. Hanson, M. Schiffer, P. Sebban, Long-range electrostatic interaction in the bacterial photosynthetic reaction centre, Nat. Struct. Biol. 2 (1995) 1057–1059.
[34] J. Tandori, L. Baciou, E. Alexov, P. Maróti, M. Schiffer, D.K. Hanson, P. Sebban, Revealing the involvement of extended hydrogen bond networks in the cooperative function between distant sites in bacterial reaction centers, J. Biol. Chem. 276 (2001) 45513–45515.
[35] H.U. Stilz, U. Finkele, W. Holzapfel, C. Lauterwasser, W. Zinth, D. Oesterhelt, Influence of M subunit Thr222 and Trp252 on quinone binding and electron transfer in *Rhodobacter sphaeroides* reaction centres, Eur. J. Biochem. 223 (1994) 233–242.
[36] W.J. Coleman, D.C. Youvan, W. Aumeier, U. Eberl, M. Volk, E. Lang, J. Siegl, R. Heckmann, W. Lersch, A. Ogrodnik, M.E. Michel-Beyerle, How conclusive is mutagenic replacement of Trp M250 in photosynthetic reaction centers?, in: M. Baltscheffsky (Ed.), Current Research in Photosynthesis, vol. 1, Kluwer Academic Publishing, Dordrecht, 1990, pp. 153–156.
[37] W.J. Coleman, E.J. Bylina, D.C. Youvan, Reconstitution of photochemical activity in *Rhodobacter capsulatus* reaction centers containing mutations at trytophan M-250 in the primary quinone binding site, in: M. Baltscheffsky (Ed.), Current Research in Photosynthesis, vol. 1, Kluwer Academic Publishing.